symmetry

MDPI

Article

Lump, Breather, Ma-Breather, Kuznetsov–Ma-Breather, Periodic Cross-Kink and Multi-Waves Soliton Solutions for Benney–Luke Equation

Miguel Vivas-Cortez [1], Sajawal Abbas Baloch [2], Muhammad Abbas [2,*], Moataz Alosaimi [3] and Guo Wei [4]

[1] Faculty of Exact and Natural Sciences, School of Physical Sciences and Mathematics, Pontifical Catholic University of Ecuador, Av. 12 de Octubre 1076 y Roca, Apartado, Quito 17-01-2184, Ecuador; mjvivas@puce.edu.ec
[2] Department of Mathematics, University of Sargodha, Sargodha 40100, Pakistan; sajawalabbasbaloch@gmail.com
[3] Department of Mathematics and Statistics, College of Science, Taif University, P.O. Box 11099, Taif 21944, Saudi Arabia; m.alosaimi@tu.edu.sa
[4] Department of Mathematics and Computer Science, University of North Carolina at Pembroke, Pembroke, NC 28372, USA; guo.wei@uncp.edu
* Correspondence: muhammad.abbas@uos.edu.pk

Abstract: The goal of this research is to utilize some ansatz forms of solutions to obtain novel forms of soliton solutions for the Benney–Luke equation. It is a mathematically valid approximation that describes the propagation of two-way water waves in the presence of surface tension. By using ansatz forms of solutions, with an appropriate set of parameters, the lump soliton, periodic cross-kink waves, multi-waves, breather waves, Ma-breather, Kuznetsov–Ma-breather, periodic waves and rogue waves solutions can be obtained. Breather waves are confined, periodic, nonlinear wave solutions that preserve their amplitude and shape despite alternating between compression and expansion. For some integrable nonlinear partial differential equations, a lump soliton is a confined, stable solitary wave solution. Rogue waves are unusually powerful and sharp ocean surface waves that deviate significantly from the surrounding wave pattern. They pose a threat to maritime safety. They typically show up in solitary, seemingly random circumstances. Periodic cross-kink waves are a particular type of wave pattern that has frequent bends or oscillations that cross at right angles. These waves provide insights into complicated wave dynamics and arise spontaneously in a variety of settings. In order to predict the wave dynamics, certain 2D, 3D and contour profiles are also analyzed. Since these recently discovered solutions contain certain arbitrary constants, they can be used to describe the variation in the qualitative characteristics of wave phenomena.

Keywords: Benney–Luke equation; lump soliton; breather waves; Ma-breather; Kuznetsov–Ma-breather; periodic cross-kink waves; multi-waves; rogue waves; periodic waves; soliton solutions

Citation: Vivas-Cortez, M.; Baloch, S.A.; Abbas, M.; Alosaimi, M.; Wei, G. Lump, Breather, Ma-Breather, Kuznetsov–Ma-Breather, Periodic Cross-Kink and Multi-Waves Soliton Solutions for Benney–Luke Equation. *Symmetry* **2024**, *16*, 747. https://doi.org/10.3390/sym16060747

Academic Editor: Natanael Karjanto

Received: 18 April 2024
Revised: 21 May 2024
Accepted: 23 May 2024
Published: 15 June 2024

1. Introduction

A fascinating feature of nature is nonlinearity, and many scientists consider nonlinear research to be the most important area of research for the fundamental understanding of nature. The investigation of multiple classes of nonlinear evolution equations (NLEEs) is essential for the mathematical modeling of complicated events that change over time. Numerous fields provide these models, such as the physical and natural sciences, neural networks, viral diseases, epidemiology, population ecology, economics and optical fibers. A few years ago, numerous innovative studies were conducted on models of the infection systems, the epidemic systems and fatal diseases in pregnant women [1,2]. Some qualitative and quantitative aspects of nonlinear phenomena can only be revealed with the help of exact solutions [3–6].

In nonlinear research, it is crucial to find exact solutions to nonlinear partial differential equations (NLPDEs). Because of their enormous importance in modeling nonlinear physical phenomena in the fields of mathematics and physics, NLEEs have received more scrutiny [7–11]. The exact solutions to NLEEs have been found using a variety of integration standards during the past few decades, including the direct algebraic scheme [12–14], the extended trial equation technique [15,16], modified $(\frac{G'}{G})$ expansion technique [17,18], the sine–cosine scheme [19,20], applications of symmetry methods to PDEs [21] and similarity methods for differential equations [22]. Some other important methods have provided exact solutions in the form of solitons, etc, like soliton molecules and Painlevé analysis for the nano-bioelectronics transmission model [23], chirp-free solitons of the Biswas–Arshed model in birefringent fibers [24], wave solutions to the unidirectional shallow water wave Dullin–Gottwald–Holm system [25,26], and solitary wave solutions for the fourth-order nonlinear Boussinesq water wave equation [27]. Özkan explored the soliton equation with the help of two efficient techniques [28]. New insights and methods in mathematical physics enable the understanding and modeling of complex physical phenomena and dynamical processes. Solitons are solitary, self-reinforcing waves that travel through a medium without changing their shape or speed. They are important in many different domains and have both theoretical and practical applications. Solitons can be helpful for studying nonlinear processes in physics because they shed light on how complex systems behave. Solitons are crucial for understanding and predicting the dynamics of ocean waves and tsunamis in water wave scenarios, which helps with the development of early warning systems. Overall, solitons are significant due to their ability to maintain stability and coherence during propagation, influencing advancements in various scientific and technical fields. Numerous soliton solutions exist, such as bell-type, kink wave, lump wave, peakons, compactons, cuspons, rogue wave, breathers, bright soliton and many more [29–31].

In mathematical physics, lump soliton solutions have attracted a lot of interest. Physical phenomena such as soliton dynamics are described by lump soliton solutions. They arise in various scientific domains, such as optic media, Bose Einstein condensate, plasma, water waves and so forth. Breather waves, sometimes referred to as soliton breathers or just breathers, are a particular kind of pulsing, localized solution to nonlinear wave equations. The oscillation pattern of these waves is periodic or quasi-periodic, gradually growing and decreasing over time without changing its general shape. Breather waves are easily distinguished from other wave types due to their characteristic features, which include well-defined width and confined amplitude peaks. To gain a deeper understanding of extreme wave events and their impact on the ecosystem, rogue waves are studied. Early warning mechanisms and maritime operations readiness are aided by this modeling. Designing coastal infrastructure, like wind turbines and oil rigs, to withstand the impact of rogue waves requires an understanding of these waves. One of the fundamental concepts in physics is periodic waves, which are recurring disturbances that oscillate regularly in space and time as they propagate through a medium. These waves include distinguishing features such as frequency, which indicates the number of full oscillations in a specific time period and is usually measured in hertz, and amplitude, which indicates the maximum deviation from the equilibrium position. A specific kind of wave phenomena known as periodic cross-kink waves is identified by frequent bends or kinks that appear along the propagation path. These waves have a distinctive pattern in which the amplitude of the wave fluctuates repeatedly in both space and time, forming kinks or cross-like structures at regular intervals. A number of factors, including boundary conditions, media qualities, and nonlinear effects, contribute to this periodic behavior.

In addition to the diverse soliton solutions of the Benney–Luke equation, similar soliton and breather-type solutions arise in other integrable systems, particularly the classical nonlinear Schrödinger (NLS) equation. In particular, the connection between the Peregrine soliton and its limiting behavior in relation to Akhmediev breathers and Kuznetsov–Ma-breathers has been explored [32,33]. Additionally, recent studies have investigated the characteristic features of the Fourier spectra of these NLS solutions [34,35].

Further exploration includes comparisons with experimental data and investigations into higher-order soliton solutions existing on a non-zero background [36,37].

In this current work, the soliton solutions of the nonlinear Benney–Luke equation (BLE) are obtained by applying some ansatz forms of solutions. We have confirmed from the literature that these solutions are new and have never been found before. Consider the Benney–Luke equation of the following form [38]

$$w_{tt} - w_{xx} + aw_{xxxx} - bw_{xxtt} + w_t w_{xx} + 2w_x w_{xt} = 0. \tag{1}$$

Equation (1) establishes a relationship between the constants $a - b = k - 1/3$, where k represents the bond number. Pego and Quintero [39] investigated the propagation of long water waves with small amplitude. They proved that the circulation of such waves in the presence of an external stiffness is governed by the Benney–Luke equation, initially derived by Benney and Luke [40]. This approach is considered to be legally valid for characterizing the bi-directional propagation of water waves under the influence of surface tension and for capturing the effects of gravitational pull [41]. The purpose of this research is to identify the lump soliton, breather waves, Kuznetsov–Ma-breather, Ma-breather, periodic cross-kink waves, multi-waves, periodic waves and rogue waves solutions for the Benney–Luke equation. The novelty of the work is in the identification of these various soliton solutions with arbitrary constants, allowing the description of qualitative variations in wave events. This work offers new insights and potential applications across various scientific and technical sectors by focusing on these specific soliton solutions and employing ansatz forms of solutions to explore the dynamics of the Benney–Luke equation.

The format of the article is as follows. The lump soliton solution will be discussed in Section 2. In Section 3, the multi-waves soliton solution will be determined. The breather waves solution is given in Section 4. The Ma-breather solution is given in Section 5. The Kuznetsov–Ma-breather solution will be found in Section 6. In Section 7, the periodic cross-kink waves solution will be discussed. In Section 8, the rogue waves solution will be obtained. In Section 9, the periodic waves solution will be obtained. Results of our recently discovered solutions are discussed in Sections 10 and 11 provides the conclusion.

2. Lump Soliton Solution

The subsequent transformation is used to find the lump soliton solution [42]:

$$w = 2(\ln f)_{xx}. \tag{2}$$

In this section, we will find lump soliton solutions of Equation (1). Lump solutions are one of multiple forms of exact solutions to NLPDEs, which are rational function solutions localized in all directions in space. The lump soliton solution of Equation (1) can be found using Equation (2), which will yield the bilinear form of the equation.

$$
\begin{aligned}
&-6f^3f_t^2f_x^2+2f^4f_{tt}f_x^1+6f^3f_x^4+20bff_t^2f_x^4-24bf^2f_{tt}f_x^4-120affx^6-72f_tf_x^6+8f^4f_tf_xf_{xt}\\
&-192bf^2f_t{f_x}^3f_{xt}+72ff{f_x}^5f_{xt}-2f^5f_{xt}^2+72bf^3f_x^2f_{xt}^2-2f^5f_xf_{xtt}+24bf^3f_x^3f_{xtt}+2f^4f_t^2f_{xx}-f^5f_{tt}f_{xx}\\
&-12f^4f_x^2f_{xx}-144bf^2f_t^2f_x^2f_{xx}+36bf^3f_{tt}f_x^2f_{xx}+360af^2f_x^4f_{xx}+180ff_tf_x^4f_{xx}+144bf^3f_tf_xf_{xt}f_{xx}\\
&-144f^2f_x^3f_{xt}f_{xx}-24bf^4f_{xt}^2f_{xx}-24bf^4f_xf_{xtt}f_{xx}+3f^5f_{xx}^2+18bf^3f_t^2f_{xx}^2-6bf^4f_{tt}f_{xx}^2-270af^3f_x^2f_{xx}^2\\
&-108f^2f_tf_x^2f_{xx}^2+48f^3f_xf_{xt}f_{xx}^2+30af^4f_{xx}^3+6f^3f_tf_{xx}^3-2f^5f_tf_{xxt}+72bf^3f_tf_x^2f_{xxt}-36f^2f_x^4f_{xxt}\\
&-48bf^4f_xf_{xt}f_{xxt}-24bf^4f_tf_{xx}f_{xxt}+60f^3f_x^2f_{xx}f_{xxt}-6f^4f_{xx}^2f_{xxt}+6bf^5f_{xxt}^2+f^6f_{xxtt}-12bf^4f_x^2f_{xxtt}\\
&+6bf^5f_{xx}f_{xxtt}+4f^5f_xf_{xxx}+24bf^3f_t^2f_xf_{xxx}-8bf^4f_{tt}f_xf_{xxx}-120af^3f_x^3f_{xxx}-48f^2f_tf_x^3f_{xxx}\\
&-16bf^4f_tf_{xt}f_{xxx}+40f^3f_x^2f_{xt}f_{xxx}+4bf^5f_{xtt}f_{xxx}+120af^4f_xf_{xx}f_{xxx}+44f^3f_tf_xf_{xx}f_{xxx}-12f^4f_{xt}f_{xx}f_{xxx}\\
&-20f^4f_xf_{xxt}f_{xxx}-10af^5f_{xxx}^2-4f^4f_tf_{xxx}^2-16bf^4f_tf_xf_{xxxt}+8f^3f_x^3f_{xxxt}+8bf^5f_{xt}f_{xxxt}-12f^4f_xf_{xx}f_{xxxt}\\
&+4f^5f_{xxx}f_{xxxt}+4bf^5f_xf_{xxxtt}-f^6f_{xxxx}-2bf^4f_t^2f_{xxxx}+bf^5f_{tt}f_{xxxx}+30af^4f_x^2f_{xxxx}+4f^3f_tf_x^2f_{xxxx}\\
&-4f^4f_xf_{xt}f_{xxxx}-15af^5f_{xx}f_{xxxx}-2f^4f_tf_{xx}f_{xxxx}+2f^5f_{xxt}f_{xxxx}+2bf^5f_tf_{xxxxt}-bf^6f_{xxxxtt}\\
&-6af^5f_xf_{xxxxx}+af^6f_{xxxxxx}=0. \qquad (3)
\end{aligned}
$$

Now, using the function f given as [43]:

$$
\begin{cases}
f=\zeta_1^2+\zeta_2^2+a_7,\\
\zeta_1=a_1x+a_2t+a_3,\\
\zeta_2=a_4x+a_5t+a_6,
\end{cases} \qquad (4)
$$

where $\zeta_1=a_1x+a_2t+a_3, \zeta_2=a_4x+a_5t+a_6$, and $1\le a_i\le 7$ are the real parameters to be found. Substitute Equation (4) into Equation (3) to obtain the specific equations that determine the values of the coefficients.

When $a_1=a_6=0$, the following solutions are obtained:

$$
a_2=\sqrt{-15}a_5, a_3=a_3, a_4=2a_5, a_5=a_5, a_7=-\frac{160}{17}aa_5^2-\frac{260}{17}a_5^2b+\frac{63}{17}a_3^2.
$$

Using the above values in Equation (2) yields

$$
w=2\frac{(\zeta_1^2+\zeta_2^2+a_7)(8{a_5}^2)-16{a_5}^2(a_5t+2a_5x)^2}{(\zeta_1^2+\zeta_2^2+a_7)^2}, \qquad (5)
$$

where

$$
\zeta_1=a_3+\mathrm{i}\sqrt{15}a_5t, \zeta_2=a_5t+2a_5x.
$$

Here, a few graphical representations of the above solution (5) are examined in the Figure 1.

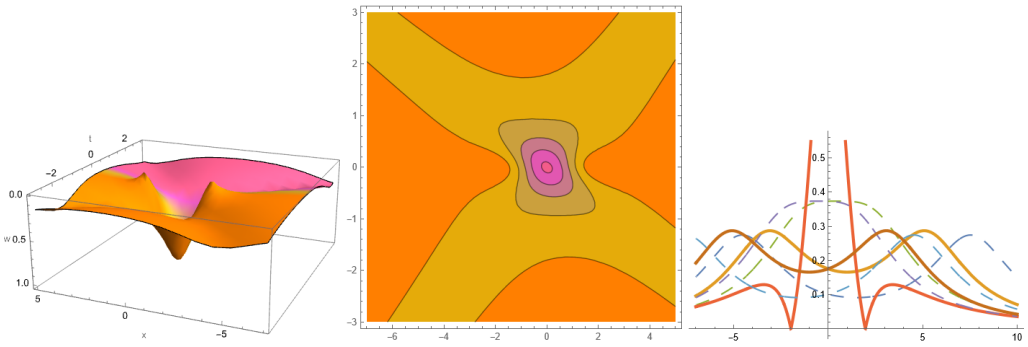

(**a**) 3D profile (**b**) Contour profile (**c**) 2D profile

Figure 1. The visual depiction for absolute part of $w(x,t)$ for Equation (5) is given. (**a**) 3D profile; (**b**) contour profile; (**c**) 2D profile, when $a_5 = -1.9$, $b = 5$, $a = 5.5$, $a_3 = 10.5$.

3. Multi-Waves Solution

In this section, we will find multi-waves solutions to (1). Much research has been conducted on multi-waves. Recently, Yousuf et al. studied the multi-wave solutions to the Kadomtsev–Petviashvili equation using two efficient techniques [44]. Wang studied the multi-wave complexiton solution, multi-wave solution and the interaction wave solutions of the (2 + 1)-dimensional Boiti–Leon–Manna–Pempinelli equation (BLMPE), which describes an irrotational incompressible fluid [45]. The following form of solution will be used for multi-waves:

$$\begin{cases} f = f_0 \cosh \zeta_1 + f_1 \cos \zeta_2 + f_2 \cosh \zeta_3 + a_{10}, \\ \zeta_1 = a_1 x + a_2 t + a_3, \\ \zeta_2 = a_4 x + a_5 t + a_6, \\ \zeta_3 = a_7 x + a_8 t + a_9, \end{cases} \tag{6}$$

where $1 \leq a_i \leq 10$ are the real parameters to be found. Substitute Equation (6) into Equation (3) to obtain the particular equations that yield values for the coefficients.

When $a_1 = a_6 = a_8 = 0$, the following solutions are obtained:

$$a_2 = \sqrt{-\frac{-32 - 985(-\frac{7}{2} + \frac{\sqrt{17}}{2})aa_7^2 - 520aa_7^2}{240a_7^2 b + 27 + 3\sqrt{17}}}, a_3 = a_3, a_4 = \frac{1}{2}\sqrt{-14 + 2\sqrt{17}}a_7,$$

$$a_5 = 0, a_7 = \frac{1}{2}\frac{\sqrt{-2b + \sqrt{-b^2 + 5b^4}}}{b}, a_9 = a_9, a_{10} = a_{10}, f_0 = f_0, f_1 = f_1, f_2 = f_2.$$

Substituting the above values in Equation (2) yields

$$w = 2\frac{\Omega\kappa_1 - \kappa_2}{\Omega^2}, \tag{7}$$

where

$$f(x,t) = \Omega = f_0 \cosh \zeta_1 + f_1 \cos \zeta_2 + f_2 \cosh \zeta_3 + a_{10},$$

$$\kappa_1 = \frac{\left(14-2\sqrt{17}\right)\left(-2b+\sqrt{-b^2+5b^4}\right)f_1 \cosh\left(\frac{\sqrt{14-2\sqrt{17}}\sqrt{-2b+\sqrt{-b^2+5b^4}}x}{4b}\right)}{16b^2} + \frac{\left(-2b+\sqrt{-b^2+5b^4}\right)f_2 \cosh\left(a_9+\frac{\sqrt{-2b+\sqrt{-b^2+5b^4}}x}{2b}\right)}{4b^2},$$

$$\kappa_2 = \left(\frac{\sqrt{14-2\sqrt{17}}\sqrt{-2b+\sqrt{-b^2+5b^4}}f_1 \sinh\left(\frac{\sqrt{14-2\sqrt{17}}\sqrt{-2b+\sqrt{-b^2+5b^4}}x}{4b}\right)}{4b} + \frac{\sqrt{-2b+\sqrt{-b^2+5b^4}}f_2 \sinh\left(a_9+\frac{\sqrt{-2b+\sqrt{-b^2+5b^4}}x}{2b}\right)}{2b} \right)^2,$$

$$\zeta_1 = a_3 + \sqrt{-\frac{-32-\frac{130a\left(-2b+\sqrt{-b^2+5b^4}\right)}{b^2}-\frac{985\left(-\frac{7}{2}+\frac{\sqrt{17}}{2}\right)a\left(-2b+\sqrt{-b^2+5b^4}\right)}{4b^2}}{27+3\sqrt{17}+\frac{60\left(-2b+\sqrt{-b^2+5b^4}\right)}{b}}}t,$$

$$\zeta_2 = \frac{i\sqrt{14-2\sqrt{17}}\sqrt{-2b+\sqrt{-b^2+5b^4}}x}{4b},$$

$$\zeta_3 = a_9 + \frac{\sqrt{-2b+\sqrt{-b^2+5b^4}}x}{2b}, \frac{-32-985(-\frac{7}{2}+\frac{\sqrt{17}}{2})aa_7^2-520aa_7^2}{240a_7^2b+27+3\sqrt{17}} < 0, -14+2\sqrt{17} > 0, -2b+\sqrt{-b^2+5b^4} > 0.$$

The graphical representations of the above solution (7) are given in Figures 2 and 3.

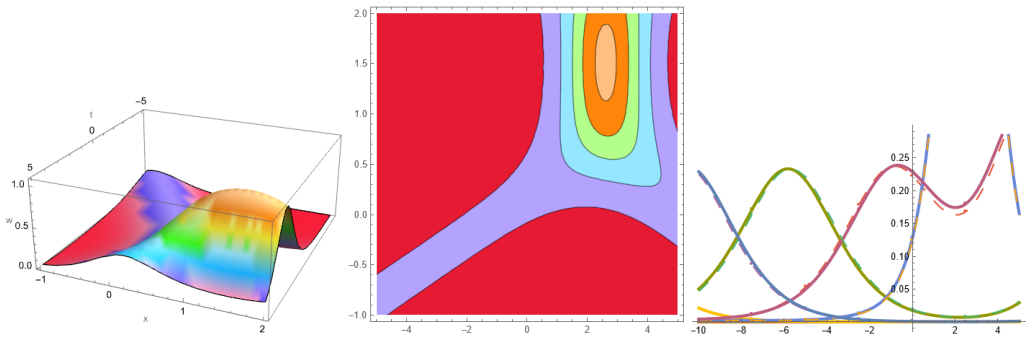

(**a**) 3D profile (**b**) Contour profile (**c**) 2D profile

Figure 2. The visual depiction of $w(x,t)$ for Equation (7) is given. (**a**) 3D profile; (**b**) contour profile; (**c**) 2D profile, when $a_{10} = -2.5$, $b = 5$, $a = -15.6$, $a_3 = -5$, $a_2 = 5$, $a_9 = -4$, $f_0 = 5$, $f_1 = 8$, $f_2 = 7$.

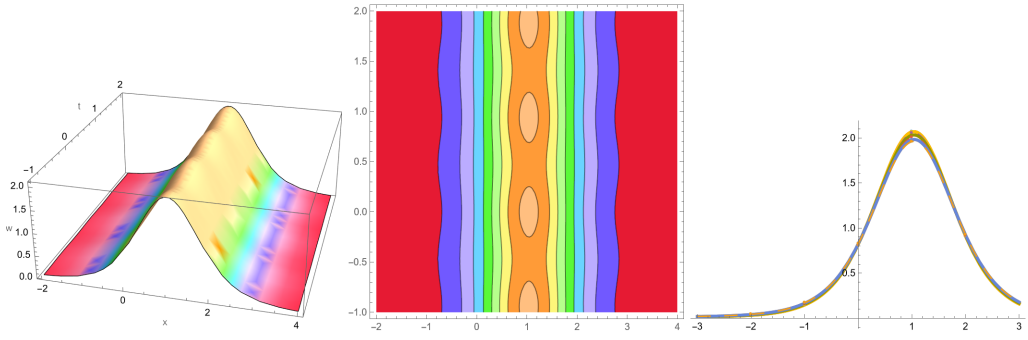

(**a**) 3D profile (**b**) Contour profile (**c**) 2D profile

Figure 3. The visual depiction of $w(x,t)$ for Equation (7) is given. (**a**) 3D profile; (**b**) contour profile; (**c**) 2D profile, when $a_{10} = 10.5$, $b = -1.5$, $a = -15.6$, $a_3 = -0.5$, $a_2 = -5$, $a_9 = 4$, $f_0 = -5$, $f_1 = 50.8$, $f_2 = 7$.

4. Breather Waves Solution

This section will provide the breather waves (BWs) solution for Equation (1). Breather waves are intriguing nonlinear wave phenomena that can be seen in a variety of physical systems. Breathers exhibit periodic oscillations in both their amplitude and width as they travel through a medium, in contrast to ordinary solitons, which are solitary waves that

maintain their shape and amplitude during propagation. The subsequent form of solution will be used for breather waves solutions:

$$\begin{cases} f(x,t) = m_1 e^{q\zeta_1(x,t)} + e^{-q\zeta_1(x,t)} + m_2 \cos(q_1\zeta_2(x,t)) + a_6, \\ \zeta_1 = a_1 x + a_2 t + a_3, \\ \zeta_2 = a_4 x + a_5 t, \end{cases} \tag{8}$$

where m_1, m_2 and a_i are real parameters to be found. By inserting Equation (8) into Equation (3), some equations that provide coefficient values are found.

When $a_2 = a_6 = 0$, the subsequent solutions are obtained:

$$a_1 = \frac{\sqrt{-\frac{1}{40a}}}{q}, a_3 = a_3, a_4 = \frac{\sqrt{\frac{8}{a}}}{8q1}, a_5 = 0, m_1 = m_1, m_2 = m_2.$$

Inserting the above values in Equation (2) yields

$$w = 2\frac{\Omega\kappa_1 - \kappa_2}{\Omega^2}, \tag{9}$$

where

$$\Omega = f(x,t) = m_1 e^{q\zeta_1(x,t)} + e^{-q\zeta_1(x,t)} + m_2 \cos(q_1\zeta_2(x,t)) + a_6,$$

$$\kappa_1 = -\frac{e^{-q\left(a_3 + \frac{\sqrt{-\frac{1}{a}}x}{2\sqrt{10}q}\right)}}{40a} - \frac{e^{q\left(a_3 + \frac{\sqrt{-\frac{1}{a}}x}{2\sqrt{10}q}\right)} m_1}{40a} - \frac{m_2 \cos\left(\frac{\sqrt{\frac{1}{a}}x}{2\sqrt{2}}\right)}{8a},$$

$$\kappa_2 = \left(-\frac{\sqrt{-\frac{1}{a}} e^{-q\left(a_3 + \frac{\sqrt{-\frac{1}{a}}x}{2\sqrt{10}q}\right)}}{2\sqrt{10}} + \frac{\sqrt{-\frac{1}{a}} e^{q\left(a_3 + \frac{\sqrt{-\frac{1}{a}}x}{2\sqrt{10}q}\right)} m_1}{2\sqrt{10}} - \frac{\sqrt{\frac{1}{a}} m_2 \sin\left(\frac{\sqrt{\frac{1}{a}}x}{2\sqrt{2}}\right)}{2\sqrt{2}} \right)^2, \zeta_1 = a_3 + \frac{\sqrt{-\frac{1}{a}}x}{2\sqrt{10}q}, \zeta_2 = \frac{\sqrt{\frac{1}{a}}x}{2\sqrt{2}q_1}.$$

Here, a few graphical representations of the above solution (9) are examined in the Figure 4.

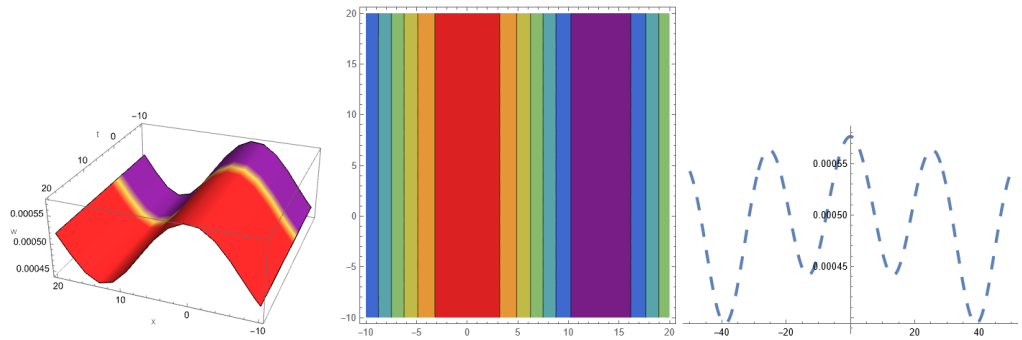

(**a**) 3D profile (**b**) Contour profile (**c**) 2D profile

Figure 4. The visual depiction of $w(x,t)$ for Equation (9) is given. (**a**) 3D profile; (**b**) contour profile; (**c**) 2D profile, when $q = 5.5$, $b = 0.9$, $a = 8.5$, $a_3 = 0.5$, $q_1 = 0.5$, $m_1 = 4$, $m_2 = 1$.

5. Ma-Breather

This section will provide the Ma-breather solution for Equation (1). The Ma-breather is a localized, explicit periodic solution. The following form of solution will be used for Ma-breather:

$$f(x,t) = e^{-i(p_1 x)} e^{k_1 t + k_2} + m_1 e^{2(k_1 t + k_2)} + e^{i(p_1 x)} + a_1, \tag{10}$$

where a_1, p_1, k_1, k_2 and m_1 are real parameters. Some equations that yield coefficient values can be obtained by inserting Equation (10) into Equation (3). The subsequent solutions are obtained:

$$a_1 = a_1, b = -\frac{100ap_1^2 + 21p_1^3\left(\frac{1}{8}p_1^3 + \frac{1}{68}\sqrt{441p_1^6 + 134400ap_1^2 + 5376}\right) + 4}{p_1^2\left(21p_1^3\left(\frac{1}{8}p_1^3 + \frac{1}{68}\sqrt{441p_1^6 + 134400ap_1^2 + 5376}\right) + 400ap_1^2 + 16\right)},$$

$$k_1 = \left(\frac{1}{8}p_1^3 + \frac{1}{68}\sqrt{441p_1^6 + 134400ap_1^2 + 5376}\right)p_1, m_1 = -\frac{1}{4}\frac{2289p_1^3\left(\frac{1}{8}p_1^3 + \frac{1}{68}\sqrt{441p_1^6 + 134400ap_1^6 + 5376}\right) + 1270ap_1^2 + 1966}{a_1^3(40ap_1^2 - 11)},$$

$$p_1 = p_1, k_2 = k_2.$$

By substituting the above values in Equation (2), we obtain

$$w = 2\frac{\Omega\kappa_1 - \kappa_2}{\Omega^2}, \tag{11}$$

where

$$\Omega = f(x,t) = e^{-i(p_1 x)} e^{k_1 t + k_2} + m_1 e^{2(k_1 t + k_2)} + e^{i(p_1 x)} + a_1,$$

$$\kappa_1 = -e^{ip_1 x} p_1^2 - e^{k_2 + p_1\left(\frac{p_1^3}{8} + \frac{1}{68}\sqrt{5376 + 134400ap_1^2 + 441p_1^6}\right)t - ip_1 x} p_1^2,$$

$$\kappa_2 = \left(ie^{ip_1 x} p_1 - ie^{k_2 + p_1\left(\frac{p_1^3}{8} + \frac{1}{68}\sqrt{5376 + 134400ap_1^2 + 441p_1^6}\right)t - ip_1 x} p_1\right)^2, 5376 + 134400ap1^2 + 441p1^6 > 0.$$

Here, a few graphical representations of the above solution (11) are examined in Figures 5 and 6.

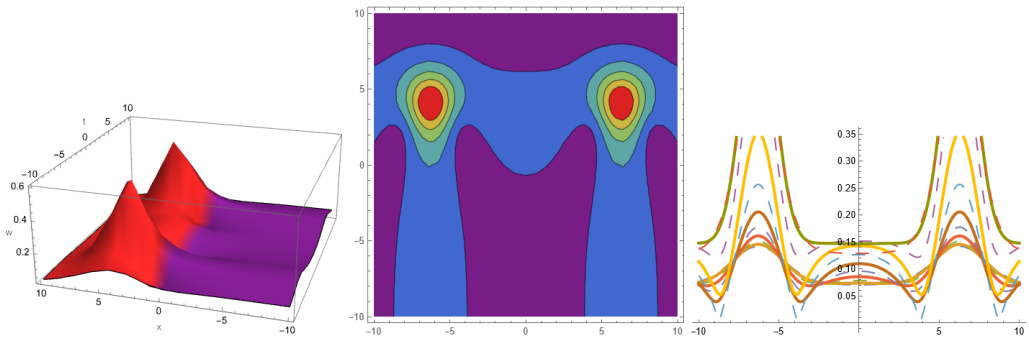

(**a**) 3D profile (**b**) Contour profile (**c**) 2D profile

Figure 5. The visual depiction of $w(x,t)$ for Equation (11) is given. (**a**) 3D profile; (**b**) contour profile; (**c**) 2D profile, when $p_1 = 0.5, k_2 = -0.5, a = -0.05, a_1 = 5.5$.

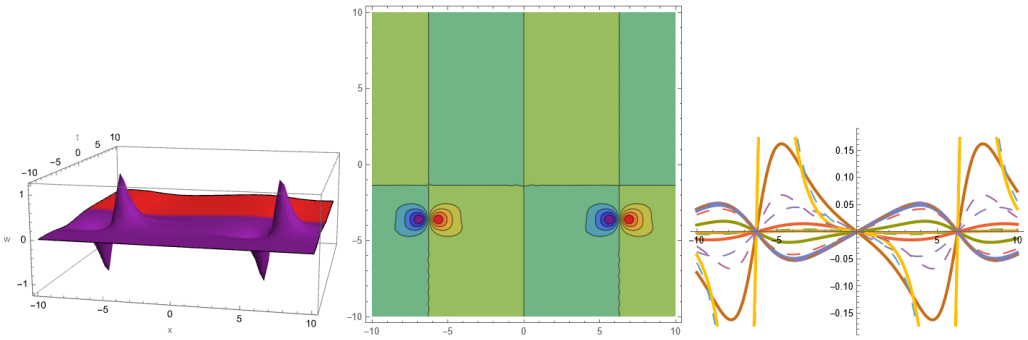

(**a**) 3D profile (**b**) Contour profile (**c**) 2D profile

Figure 6. The visual depiction of $w(x,t)$ for Equation (11) is given. (**a**) 3D profile; (**b**) contour profile; (**c**) 2D profile, when $p_1 = -0.5, k_2 = -1.5, a = 0.5, a_1 = 10$.

6. Kuznetsov–Ma-Breather

The Kuznetsov–Ma-breather is an explicit time-periodic solution. The following form of solution will be used for Kuznetsov–Ma-breather:

$$f(x,t) = \mathrm{e}^{-p_1(x-b_1 t)} + a_1 \cos(p(x+b_1 t)) + a_2 \cos(p(x-b_1 t)), \tag{12}$$

where a_1, p_1, p, a_2 and b_1 are real parameters. Some equations that yield coefficient values can be obtained by inserting Equation (12) into Equation (3). The subsequent solutions are obtained:

$$a_1 = a_1, a_2 = a_2, p = \sqrt{-\frac{1}{32}\frac{3-\frac{1}{2}\frac{5a+3b+\sqrt{25a^2+2ab+9b^2}}{b}}{a}}, b_1 = \frac{1}{\sqrt{2}}\sqrt{\frac{5a+3b+\sqrt{25a^2+2ab+9b^2}}{b}}, p_1 = 0.$$

By substituting the above values in Equation (2), we obtain

$$w = 2\frac{\Omega\kappa_1 - \kappa_2}{\Omega^2}, \tag{13}$$

where

$$\Omega = f(x,t) = \mathrm{e}^{-p_1(x-b_1 t)} + a_1 \cos(p(x+b_1 t)) + a_2 \cos(p(x-b_1 t)),$$

$$\kappa_1 = \frac{a_2\left(3-\frac{\lambda}{2}\right)\cos\left(\frac{\sqrt{-\frac{3-\frac{\lambda}{2}}{a}}\left(-\frac{\sqrt{\lambda}t}{\sqrt{2}}+x\right)}{4\sqrt{2}}\right)}{32a} + \frac{a_1\left(3-\frac{\lambda}{2}\right)\cos\left(\frac{\sqrt{-\frac{3-\frac{\lambda}{2}}{a}}\left(\frac{\sqrt{\lambda}t}{\sqrt{2}}+x\right)}{4\sqrt{2}}\right)}{32a},$$

$$\kappa_2 = \left(-\frac{a_2\sqrt{-\frac{3-\frac{\lambda}{2}}{a}}\sin\left(\frac{\sqrt{-\frac{3-\frac{\lambda}{2}}{a}}\left(-\frac{\sqrt{\lambda}t}{\sqrt{2}}+x\right)}{4\sqrt{2}}\right)}{4\sqrt{2}} - \frac{a_1\sqrt{-\frac{3-\frac{\lambda}{2}}{a}}\sin\left(\frac{\sqrt{-\frac{3-\frac{\lambda}{2}}{a}}\left(\frac{\sqrt{\lambda}t}{\sqrt{2}}+x\right)}{4\sqrt{2}}\right)}{4\sqrt{2}}\right)^2,$$

$$\lambda = \frac{5a+3b+\sqrt{25a^2+2ab+9b^2}}{b}, 25a^2+2ab+9b^2 > 0.$$

Here, a few graphical representations of the above solution (13) are given in Figures 7 and 8.

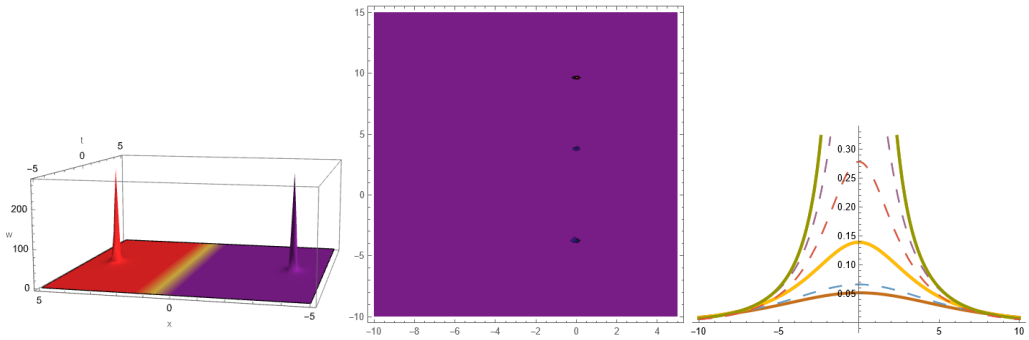

(**a**) 3D profile (**b**) Contour profile (**c**) 2D profile

Figure 7. The visual depiction of $w(x,t)$ for Equation (13) is given. (**a**) 3D profile; (**b**) contour profile; (**c**) 2D profile, when $b=-6, a=10, a_2=-0.5, a_1=5.5$.

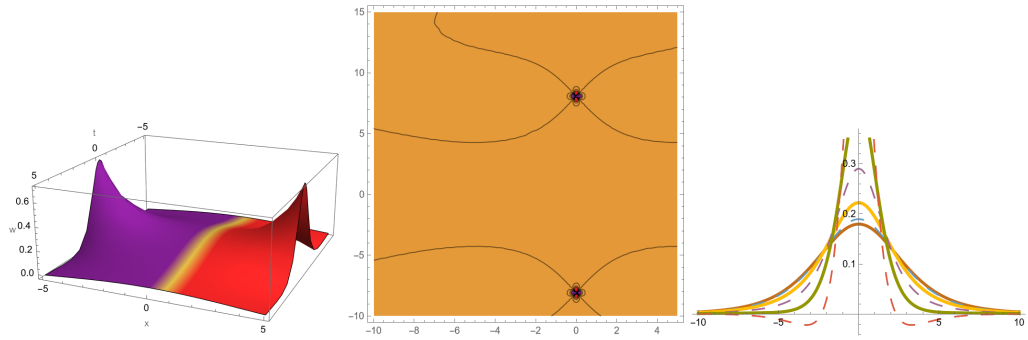

(**a**) 3D profile (**b**) Contour profile (**c**) 2D profile

Figure 8. The visual depiction of $w(x,t)$ for Equation (13) is given. (**a**) 3D profile; (**b**) contour profile; (**c**) 2D profile, when $b=-6, a=1, a_2=-0.5, a_1=5.5$.

7. Periodic Cross-Kink Waves Solution

The periodic cross-kink waves (PCKWs) solution for Equation (1) is given in this section. The following form of solution will be used for the PCKWs solution:

$$\begin{cases} f(x,t) = m_1 e^{\zeta_1} + e^{-\zeta_1} + m_2 \cos(\zeta_2(x,t)) + m_3 \cosh(\zeta_3(x,t)) + a_{10}, \\ \zeta_1 = a_1 x + a_2 t + a_3, \\ \zeta_2 = a_4 x + a_5 t, \\ \zeta_3 = a_6 x + a_7 t. \end{cases} \tag{14}$$

Some equations that provide coefficient values can be obtained by inserting Equation (14) into Equation (3).

When $a_1 = 0, a_3 = 0, a_7 = 0, m_1 = 0$, the following solutions are obtained:

$$a_2 = \frac{1026000a^2b + 311070a - 167179b}{205200a^2}, a_4 = \sqrt{\frac{1}{8a}}, a_5 = 0, a_6 = \sqrt{-\frac{47}{120a}}, a_{10} = a_{10}, m_2 = m_2, m_3 = m_3.$$

Substituting the above values in Equation (2) yields

$$w = 2\frac{\Omega\kappa_1 - \kappa_2}{\Omega^2}, \tag{15}$$

where

$$\Omega = f(x,t) = m_1 e^{\zeta_1} + e^{-\zeta_1} + m_2 \cos(\zeta_2(x,t)) + m_3 \cosh(\zeta_3(x,t)) + a_{10},$$

$$\kappa_1 = -\frac{m_2 \cos\left(\frac{\sqrt{\frac{1}{a}}x}{2\sqrt{2}}\right)}{8a} - \frac{47m_3 \cosh\left(\frac{1}{2}\sqrt{\frac{47}{30}}\sqrt{-\frac{1}{a}}x\right)}{120a}, \kappa_2 = -\frac{m_2 \cos\left(\frac{\sqrt{\frac{1}{a}}x}{2\sqrt{2}}\right)}{8a} - \frac{47m_3 \cosh\left(\frac{1}{2}\sqrt{\frac{47}{30}}\sqrt{-\frac{1}{a}}x\right)}{120a},$$

$$\zeta_1 = \frac{(311070a - 167179b + 1026000a^2b)t}{205200a^2}, \zeta_2 = \frac{\sqrt{\frac{1}{a}}x}{2\sqrt{2}}, \zeta_3 = \frac{1}{2}\sqrt{-\frac{47}{30a}}.x$$

The graphical representations of the above solution (15) are displayed in Figures 9 and 10.

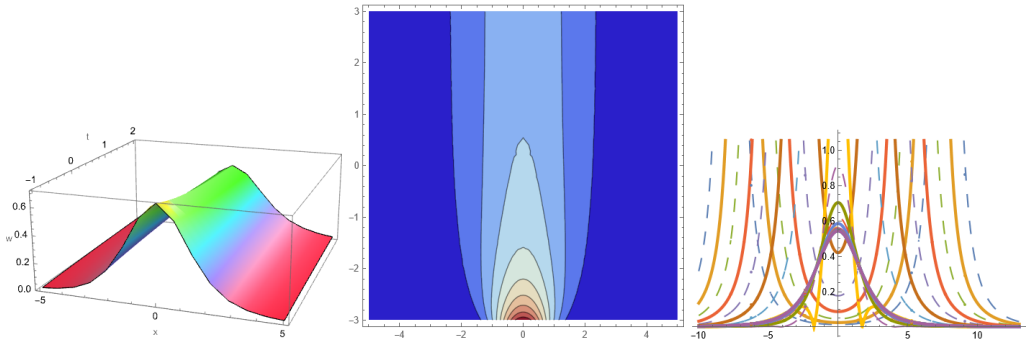

(**a**) 3D profile (**b**) Contour profile (**c**) 2D profile

Figure 9. The visual depiction of $w(x,t)$ for Equation (15) is given. (**a**) 3D profile; (**b**) contour profile; (**c**) 2D profile, when $a_{10} = 1.5$, $b = 0.5$, $a = -1$, $m_2 = -1.3$, $m_3 = -5$.

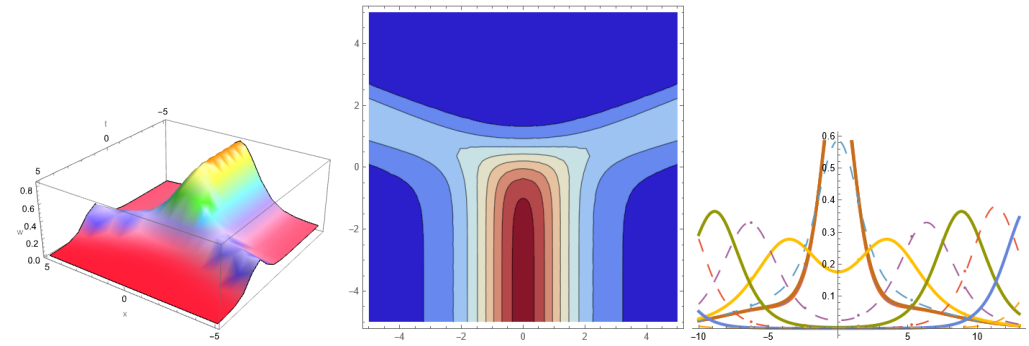

(**a**) 3D profile (**b**) Contour profile (**c**) 2D profile

Figure 10. The visual depiction of $w(x,t)$ for Equation (15) is given. (**a**) 3D profile; (**b**) contour profile; (**c**) 2D profile, when $a_{10} = -0.5$, $b = 0.5$, $a = -0.5$, $m_2 = 2.3$, $m_3 = 0.5$.

8. Rogue Waves

This section will provide the rogue waves solution for Equation (1). In order to comprehend extreme wave events and their effects on the ecosystem more fully, the rogue waves are investigated. The following form of solution will be used for rogue waves:

$$\begin{cases} f(x,t) = \zeta_1^2 + \zeta_2^2 + m_1 \cosh(\alpha(x,t)) + a_7, \\ \zeta_1 = a_1 x + a_2 t + a_3, \\ \zeta_2 = a_4 x + a_5 t + a_6, \\ \alpha(x,t) = b_1 x + b_2 t, \end{cases} \tag{16}$$

where $1 \leq a_i \leq 7$, b_1, b_2 and m_1 are real parameters to be found. By inserting Equation (16) into Equation (3), one can obtain particular equations that provide values for parameters.

When $a_1 = b_2 = a_6 = 0$, we obtain the following solutions:

$$a_2 = \sqrt{-\frac{378aa_4^2 + 81aa_5^2 - 108a_5^2 b}{3a - 4b}}, a_3 = a_3, a_5 = a_5, a_7 = a_7, m_1 = m_1, b_1 = \sqrt{\frac{2}{3a}}.$$

Substituting the above values in Equation (2) yields

$$w = 2\frac{\Omega\kappa_1 - \kappa_2}{\Omega^2}, \tag{17}$$

where

$$f(x,t) = \Omega = \zeta_1^2 + \zeta_2^2 + m_1 \cosh(\alpha(x,t)) + a_7,$$

$$\kappa_1 = 2a_4^2 + \frac{2m_1 \cosh\left(\sqrt{\frac{2}{3}}\sqrt{\frac{1}{a}}x\right)}{3a}, \kappa_2 = \left(2a_4(a_5 t + a_4 x) + \sqrt{\frac{2}{3}}\sqrt{\frac{1}{a}} m_1 \sinh\left(\sqrt{\frac{2}{3}}\sqrt{\frac{1}{a}}x\right)\right)^2,$$

$$\zeta_1 = a_3 + \sqrt{-\frac{378aa_4^2 + 81aa_5^2 - 108a_5^2 b}{3a - 4b}}t, \zeta_2 = a_5 t + a_4 x, \alpha(x,t) = \sqrt{\frac{2}{3a}}x, \frac{378aa4^2 + 81aa5^2 - 108a5^2 b}{3a - 4b} < 0.$$

The graphical representations of the above solution (17) are displayed in Figures 11 and 12.

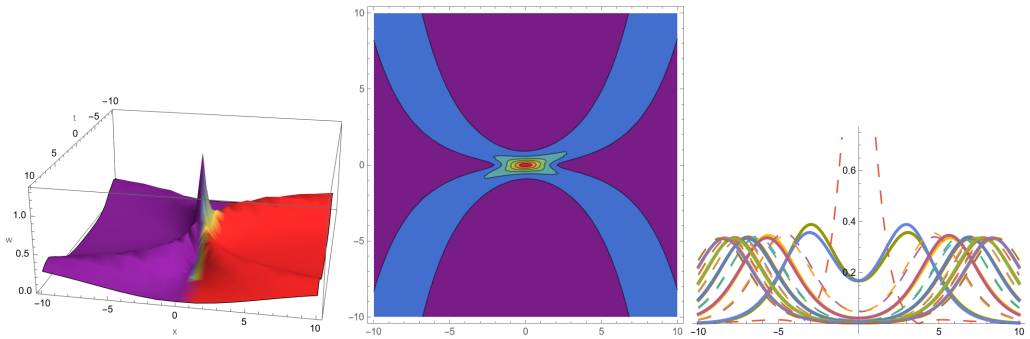

(**a**) 3D profile (**b**) Contour profile (**c**) 2D profile

Figure 11. The visual depiction of $w(x,t)$ for Equation (17) is given. (**a**) 3D profile; (**b**) contour profile; (**c**) 2D profile, when $a4 = 0.5, a_7 = 0.5, m_1 = -5, b = -0.3, a_5 = 0.5, a = 1, a_3 = -0.5$.

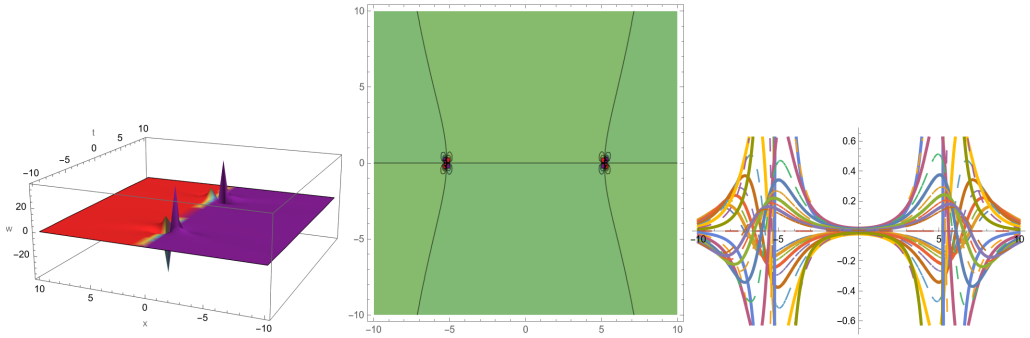

(**a**) 3D profile (**b**) Contour profile (**c**) 2D profile

Figure 12. The visual depiction of $w(x,t)$ for Equation (17) is given. (**a**) 3D profile; (**b**) contour profile; (**c**) 2D profile, when $a_4 = -0.5, a_7 = -5.5, m_1 = -5.5, b = -5, a_5 = -0.5, a = 0.9, a_3 = 15.5$.

9. Periodic Waves Solution

This section will provide the periodic waves solution for Equation (1). For this, we study the following form of the solution.

$$\begin{cases} f(x,t) = \zeta_1^2 + \zeta_2^2 + m_1 \cos(\alpha(x,t)) + a_7, \\ \zeta_1 = a_1 x + a_2 t + a_3, \\ \zeta_2 = a_4 x + a_5 t + a_6, \\ \alpha(x,t) = b_1 x + b_2 t, \end{cases} \tag{18}$$

where a_i, b_i and m_1 are the real constants that need to be found. By substituting Equation (10) into Equation (3), we attain following values of parameters.

When $a_3 = a_4 = a_7 = b_2 = 0$, we obtain the following solutions:

$$a_1 = \sqrt{\frac{32b - 49b_1^4}{360a}} a_5, a_2 = \frac{a_5}{\sqrt{3}}, a_5 = a_5, a_6 = \frac{14}{3} a_5 b_1^2, b_1 = b_1.$$

By using the above values in Equation (2), we obtain

$$w = 2\frac{\Omega\kappa_1 - \kappa_2}{\Omega^2}, \tag{19}$$

where

$$f(x,t) = \Omega = \zeta_1(x,t)^2 + \zeta_2(x,t)^2 + m_1 \cos(\alpha(x,t)) + a_7,$$

$$\kappa_1 = \frac{33320 a_5^2 b_1^4}{27b^2} - \frac{1}{2} a^2 m_1 \cos\left(\frac{ax}{\sqrt{2}}\right),$$

$$\kappa_2 = \left(\frac{28\sqrt{\frac{85}{3}} a_5 b_1^2 \left(\frac{14i\sqrt{85} a_5 b_1^2 t}{3b} + \frac{14\sqrt{\frac{85}{3}} a5 b_1^2 x}{3b} \right)}{3b} - \frac{a m_1 \sin\left(\frac{ax}{\sqrt{2}}\right)}{\sqrt{2}} \right)^2,$$

$$\zeta_1 = \frac{a_5 t}{\sqrt{3}} + \frac{a_5 \sqrt{\frac{32b - 49b_1^4}{a}} x}{6\sqrt{10}}, \zeta_2 = \frac{14 a_5 b_1^2}{3} + a_5 t, \alpha = b_1 x, \frac{32b - 49b_1^4}{360a} > 0.$$

Here, a few graphical representations of the above solution (19) are displayed in Figures 13 and 14.

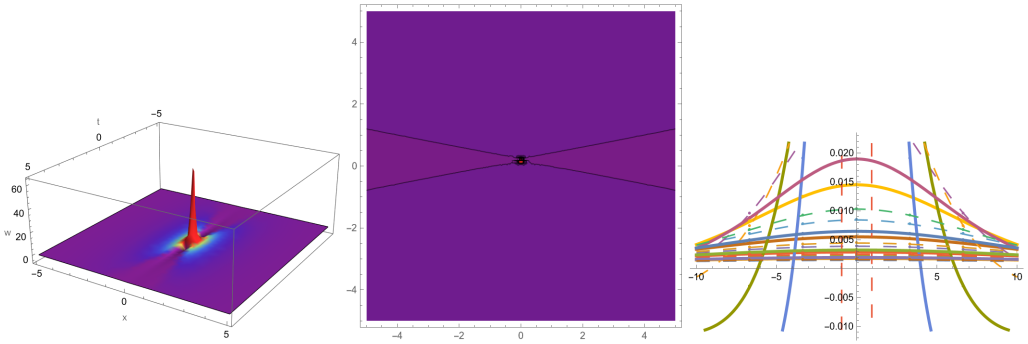

(**a**) 3D profile (**b**) Contour profile (**c**) 2D profile

Figure 13. The visual depiction of $w(x,t)$ for Equation (19) is given. (**a**) 3D profile; (**b**) contour profile; (**c**) 2D profile, when $a = -5, b = -5, a_5 = -5, b_1 = -5, m_1 = 0.5$.

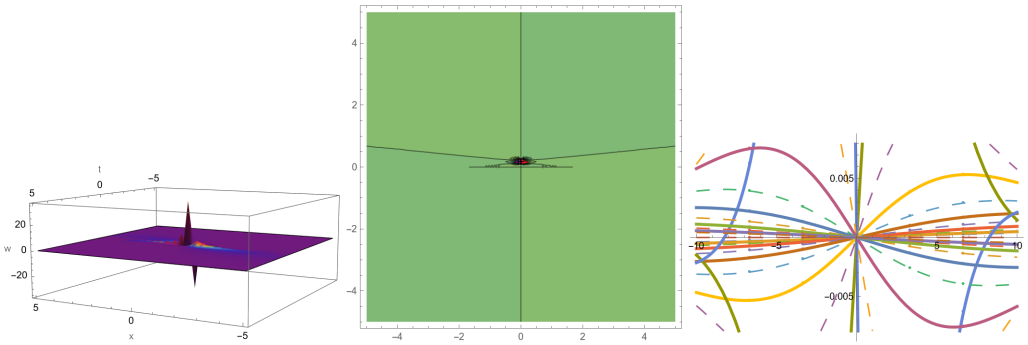

(**a**) 3D profile (**b**) Contour profile (**c**) 2D profile

Figure 14. The visual depiction of $w(x,t)$ for Equation (19) is given. (**a**) 3D profile; (**b**) contour profile; (**c**) 2D profile, when $a = -0.5, b = -5, a_5 = -5, b_1 = -5, m_1 = -0.5$.

10. Results and Discussion

The Benney–Luke equation is used in many different studies. For example, exact solutions to the BLE were found by utilizing the enhanced (G'/G) technique [46]. The homogeneous balancing technique was utilized to obtain the exact solutions for the BLE [47], while the ansatz method was employed to find the shock wave solution for the BLE [48]. Additionally, much research has been carried out on the Benney–Luke equation [49–51]. In our study, we employed various ansatz forms of solutions to investigate the Benney–Luke equation, focusing on lump soliton, rogue waves, breather waves, Kuznetsov–Ma-breather, Ma-breather and periodic cross-kink wave solutions.

The lump soliton, rogue waves, breather waves, Kuznetsov–Ma-breather, Ma-breather and periodic cross-kink waves solutions are obtained for various parameter values using Mathematica 13.2. The lump soliton solution is shown by Equation (5). These solitons have been explored in various physical occurrences, including optical media, plasma, shallow water waves and similar phenomena. Equation (7) illustrates the solution for multi-waves. Complex wave patterns that are defined by the simultaneous existence of several different wave components propagating across a material are referred to as multi-waves. These waves can have a variety of amplitudes, wavelengths and frequencies, which can lead to complex interference patterns and nonlinear interactions. Equation (9) shows the breather waves solution. Breather waves, sometimes referred to as soliton waves or localized waves, are unified, consistent wave solutions that travel through a medium while retaining their amplitude and form, frequently in the face of dispersion and nonlinearity. Breather waves are important in the study of wave dynamics, such as in oceanography for modeling rogue waves or in plasma physics for understanding wave–particle interactions. Breather waves are used in many different domains, such as nonlinear optics, where they allow ultrashort pulses to be generated for imaging and high-speed communication systems. Equation (11) illustrates the Ma-breather solution. This solution can be relevant in the study of wave stability and interactions, particularly in nonlinear systems where breather-like structures emerge. The Kuznetsov–Ma-breather solution is shown by Equation (13).

The solution for periodic cross-kink waves is represented by Equation (15). These waves, commonly observed in nonlinear systems such as plasmas, magnetic materials or elastic structures, exhibit unified and persistent wave patterns characterized by periodic oscillations in multiple dimensions. Periodic cross-kink waves originate from the interaction of dispersion, nonlinearity and inherent features of the medium. They are controlled by nonlinear equations. These solutions are helpful for comprehending interference effects and wave patterns in several mediums, such acoustic wave propagation or crystal lattice dynamics. The solution for rogue waves is given by Equation (17). Rogue waves, which are exceptionally large and unexpected ocean waves, emerge suddenly amidst a sea of smaller waves. These waves, sometimes referred to as freak waves or monster waves, frequently tower over surrounding waves and reach heights noticeably higher than the average waves in the the area. While rogue waves are typically associated with mar-

itime hazards, they also hold value in oceanography, for enhancing our comprehension of climatic patterns and predictive models. Furthermore, research on rogue waves drives advancements in maritime engineering, renewable energy technologies and communications, with potential applications spanning from robust infrastructure design to efficient signal processing, and renewable energy generation. The periodic waves solution is represented by Equation (19). The lump soliton solution is depicted in Figure 1. It depicts the 3D, contour and 2D profiles for the absolute part of w, illustrating a dark face of lump solution for $a_5 = -1.9$, $b = 5$, $a = 5.5$ and $a_3 = 10.5$. Figure 2 depicts the 3D, contour and 2D profiles of w, illustrating the large peak wave for $a_{10} = -2.5$, $b = 5$, $a = -15.6$, $a_3 = -5$, $a_2 = 5$, $a_9 = -4$, $f_0 = 5$, $f_1 = 8$ and $f_2 = 7$. Figure 3 depicts the 3D, contour and 2D profiles of w, illustrating a large bright soliton solution for $a_{10} = 10.5$, $b = -1.5$, $a = -15.6$, $a_3 = -0.5$, $a_2 = -5$, $a_9 = 4$, $f_0 = -5$, $f_1 = 50.8$ and $f_2 = 7$. Figure 4 shows the 3D, contour and 2D profiles of w, illustrating a periodic wave solution for $q = 5.5$, $b = 0.9$, $a = 8.5$, $a_3 = 0.5$,$q_1 = 0.5$, $m_1 = 4$ and $m_2 = 1$. Figure 5 depicts the 3D, contour and 2D profiles of w, illustrating two bright faces of solution for $p_1 = 0.5$, $k_2 = -0.5$, $a = -0.05$ and $a_1 = 5.5$.

Figure 6 shows the 3D, contour and 2D profiles of w, illustrating two bright and two dark faces of solution for $p_1 = -0.5$, $k_2 = -1.5$, $a = 0.5$ and $a_1 = 10$. Figure 7 depicts the 3D plot, contour plot and 2D graphs of w, illustrating two bright faces of solution for $b = -6$, $a = 10$, $a_2 = -0.5$ and $a_1 = 5.5$. In Figure 8 depicts the 3D, contour and 2D profiles of w, illustrating a large bright soliton solution for $b = -6$, $a = 1$, $a_2 = -0.5$ and $a_1 = 5.5$. Figures 9 and 10 depict the 3D, contour and 2D profiles of w, illustrating a bright soliton solution for $a_{10} = 1.5$, $b = 0.5$, $a = -1$, $m_2 = -1.3$, $m_3 = -5$, and $a_{10} = -0.5$, $b = 0.5$, $a = -0.5$, $m_2 = 2.3$, $m_3 = 0.5$, respectively. Figure 11 depicts the 3D, contour and 2D profiles of w, illustrating a bright face of solution for $a4 = 0.5$, $a_7 = 0.5$,$m_1 = -5$, $b = -0.3$, $a_5 = 0.5$, $a = 1$ and $a_3 = -0.5$. Figure 12 shows the 3D, contour and 2D profiles of w, illustrating multiple dark and bright faces of solution for $a_4 = -0.5$, $a_7 = -5.5$, $m_1 = -5.5$, $b = -5$,$a_5 = -0.5$, $a = 0.9$ and $a_3 = 15.5$. Figure 13 shows the 3D plot, contour plot and 2D graphs of w, illustrating a bright face of solution for $a = -5$, $b = -5$, $a_5 = -5$, $b_1 = -5$ and $m_1 = 0.5$. Figure 14 depicts the 3D plot, contour plot and 2D graphs of w, illustrating one bright and one dark face of solution for $a = -0.5$, $b = -5$, $a_5 = -5$, $b_1 = -5$ and $m_1 = -0.5$.

11. Conclusions

The main objective of this work is to explore the exact solutions of the Benney–Luke equation (BLE). This study utilizes ansatz forms of solutions to introduce and examine various types of solitons, including lump soliton, breather waves, Ma-breather, Kuznetsov–Ma-breather, multi-waves, periodic cross-kink waves, periodic waves and rogue waves solutions to the BLE. Solitons play a crucial role in many areas, including biological systems and optical communications. Their self-sustaining, stable waveforms resist dispersion, allowing for long-distance information transmission and fostering strong signal integrity in complicated media. The found solutions are said to be novel, intriguing and noteworthy, covering a significantly wider range of free constants. They may be helpful in characterizing and elucidating the underlying structures of complex behaviors that are seen in the natural world. We set the free parameters to appropriate values and produce a variety of 3D, 2D and contour profiles to physically represent the solutions that we have found. The aim of this work is to find previously undiscovered, newly determined solitons for the Benney–Luke equation. Researchers can explore new phenomena, patterns and interactions between solitons to find novel soliton solutions. In domains like communication systems or marine engineering, concentrating on practical applications could encourage research toward practical solutions. Advancing the study of soliton solutions in the Benney–Luke equation requires collaboration, interdisciplinary work, and the use of advanced computational and experimental techniques. Upon reviewing the literature, we have concluded that our documented results represent a novel contribution to the field. This could inspire scientists and scholars to further research this topic and enhance our understanding.

Author Contributions: M.V.-C.: software, visualization, writing–review & editing. S.A.B.: conceptualization, methodology, writing–original draft. M.A. (Muhammad Abbas): formal analysis, software, supervision, investigation, visualization, writing–original draft, writing–review & editing. M.A. (Moataz Alosaimi): formal analysis, investigation, writing–original draft, writing–review & editing. G.W.: formal analysis, investigation, visualization, writing—original draft, writing–review & editing. All authors have read and agreed to the published version of the manuscript.

Funding: This research was funded by Deanship of Graduate Studies and Scientific Research, Taif University.

Data Availability Statement: The data and materials used to support the findings of this study are included in this article.

Acknowledgments: The authors would like to acknowledge Deanship of Graduate Studies and Scientific Research, Taif University for funding this work.

Conflicts of Interest: The authors confirm that they have no relevant financial or non-financial competing interests. All the authors with the consultation of each other completed this research and drafted the manuscript together. All authors have read and approved the final manuscript.

References

1. Gao, W.; Günerhan, H.; Baskonus, H.M. Analytical and approximate solutions of an epidemic system of HIV/AIDS transmission. *Alex. Eng. J.* **2020**, *59*, 3197–3211. [CrossRef]
2. Gao, W.; Günerhan, H.; Baskonus, H.M. Novel Dynamic Structures of 2019-nCoV with Nonlocal Operator via Powerful Computational Technique. *Biology* **2020**, *9*, 107. [CrossRef] [PubMed]
3. Ablowitz, M.J.; Clarkson, P.A. *Solitons, Nonlinear Evolution Equations and Inverse Scattering*; Cambridge University Press: London, UK, 1991; Volume 149.
4. Chen, S.J.; Yin, Y.H.; Ma, W.X.; Lü, X. Abundant exact solutions and interaction phenomena of the (2+ 1)-dimensional YTSF equation. *Anal. Math. Phys.* **2019**, *9*, 2329–2344. [CrossRef]
5. Hua, Y.F.; Guo, B.L.; Ma, W.X.; Lü, X. Interaction behavior associated with a generalized (2+ 1)-dimensional Hirota bilinear equation for nonlinear waves. *Appl. Math. Model.* **2019**, *74*, 184–198. [CrossRef]
6. Lu, X.; Ma, W.X.; Yu, J.; Lin, F.; Khalique, C.M. Envelope bright-and dark-soliton solutions for the Gerdjikov–Ivanov model. *Nonlinear Dyn.* **2015**, *82*, 1211–1220. [CrossRef]
7. Tran, M.Q. Ion acoustic solitons in a plasma A review of their experimental properties and related theories. *Phys. Scr.* **1979**, *20*, 317. [CrossRef]
8. Seadawy, A.R. Stability analysis for two-dimensional ion-acoustic waves in quantum plasmas. *Phys. Plasmas* **2014**, *21*, 052107. [CrossRef]
9. Seadawy, A.R. Three-dimensional nonlinear modified Zakharov–Kuznetsov equation of ion-acoustic waves in a magnetized plasma. *Comput. Math. Appl.* **2016**, *71*, 201–212. [CrossRef]
10. Yildirim, O. On the unique weak solvability of second-order unconditionally stable difference scheme for the system of sine-Gordon equations. *Nonlinear Anal. Model. Control* **2024**, *29*, 244–264. [CrossRef]
11. Yildirim, Ö.; Uzun, M. Weak solvability of the unconditionally stable difference scheme for the coupled sine-Gordon system. *Nonlinear Anal.-Model. Control* **2020**, *25*, 997–1014. [CrossRef]
12. Hereman, W.; Banerjee, P.P.; Korpel, A.; Assanto, G.; Van Immerzeele, A.; Meerpoel, A. Exact solitary wave solutions of nonlinear evolution and wave equations using a direct algebraic method. *J. Phys. Math. Gen.* **1986**, *19*, 607. [CrossRef]
13. Hubert, M.B.; Betchewe, G.; Justin, M.; Doka, S.Y.; Crepin, K.T.; Biswas, A.; Belic, M. Optical solitons with Lakshmanan–Porsezian–Daniel model by modified extended direct algebraic method. *Optik* **2018**, *162*, 228–236. [CrossRef]
14. Tian, Y.; Liu, J. Direct algebraic method for solving fractional Fokas equation. *Therm. Sci.* **2021**, *25*, 2235–2244. [CrossRef]
15. Gurefe, Y.; Misirli, E.; Sonmezoglu, A.; Ekici, M. Extended trial equation method to generalized nonlinear partial differential equations. *Appl. Math. Comput.* **2013**, *219*, 5253–5260.
16. Ekici, M.; Mirzazadeh, M.; Sonmezoglu, A.; Ullah, M.Z.; Zhou, Q.; Moshokoa, S.P.; Belic, M. Nematicons in liquid crystals by extended trial equation method. *J. Nonlinear Opt. Phys. Mater.* **2017**, *26*, 1750005. [CrossRef]
17. Yu-Bin, Z.; Chao, L. Application of modified $(\frac{G'}{G})$-expansion method to traveling wave solutions for Whitham–Broer–Kaup-like equations.*Commun. Theor. Phys.* **2009**, *51*, 664. [CrossRef]
18. Shehata, A.R. The traveling wave solutions of the perturbed nonlinear Schrödinger equation and the cubic–quintic Ginzburg Landau equation using the modified $(\frac{G'}{G})$-expansion method. *Appl. Math. Comput.* **2010**, *217*, 1–10. [CrossRef]
19. Wazwaz, A.M. A sine-cosine method for handlingnonlinear wave equations. *Math. Comput. Model.* **2004**, *40*, 499–508. [CrossRef]
20. Bekir, A. New solitons and periodic wave solutions for some nonlinear physical models by using the sine–cosine method. *Phys. Scr.* **2008**, *77*, 045008. [CrossRef]
21. Bluman, G.W.; Cheviakov, A.F.; Anco, S.C. *Applications of Symmetry Methods to Partial Differential Equations*; Springer: New York, NY, USA, 2009.
22. Bluman, G.W.; Cole, J.D. *Similarity Methods for Differential Equations*; Springer: New York, NY, USA, 1974.

23. Farah, N.; Seadawy, A.R.; Ahmad, S.; Rizvi, S.T.R.; Younis, M. Interaction properties of soliton molecules and Painleve analysis for nano bioelectronics transmission model. *Opt. Quantum Electron.* **2020**, *52*, 1–15. [CrossRef]
24. Rizvi, S.T.R.; Seadawy, A.R.; Ali, I.; Bibi, I.; Younis, M. Chirp-free optical dromions for the presence of higher order spatio-temporal dispersions and absence of self-phase modulation in birefringent fibers. *Mod. Phys. Lett. B* **2020**, *34*, 2050399. [CrossRef]
25. Bilal, M.; Seadawy, A.R.; Younis, M.; Rizvi, S.T.R.; Zahed, H. Dispersive of propagation wave solutions to unidirectional shallow water wave Dullin–Gottwald–Holm system and modulation instability analysis. *Math. Methods Appl. Sci.* **2021**, *44*, 4094–4104. [CrossRef]
26. Younas, U.; Seadawy, A.R.; Younis, M.; Rizvi, S.T.R. Dispersive of propagation wave structures to the Dullin–Gottwald–Holm dynamical equation in a shallow water waves. *Chin. J. Phys.* **2020**, *68*, 348–364. [CrossRef]
27. Helal, M.A.; Seadawy, A.R.; Zekry, M.H. Stability analysis of solitary wave solutions for the fourth-order nonlinear Boussinesq water wave equation. *Appl. Math. Comput.* **2014**, *232*, 1094–1103. [CrossRef]
28. Özkan, A. Analytical solutions of the nonlinear (2+ 1)-dimensional soliton equation by using some methods. *J. Eng. Technol. Appl. Sci.* **2022**, *7*, 141–155. [CrossRef]
29. Rao, J.; Mihalache, D.; Cheng, Y.; He, J. Lump-soliton solutions to the Fokas system. *Phys. Lett. A* **2019**, *383*, 1138–1142. [CrossRef]
30. Liu, J.; Zhang, Y. Construction of lump soliton and mixed lump stripe solutions of (3+ 1)-dimensional soliton equation. *Results Phys.* **2018**, *10*, 94–98. [CrossRef]
31. Abdullah; Seadawy, A.R.; Wang, J. Three-dimensional nonlinear extended Zakharov-Kuznetsov dynamical equation in a magnetized dusty plasma via acoustic solitary wave solutions. *Braz. J. Phys.* **2019**, *49*, 67–78. [CrossRef]
32. Karjanto, N. Peregrine soliton as a limiting behavior of the Kuznetsov-Ma and Akhmediev breathers. *Front. Phys.* **2021**, *9*, 599767. [CrossRef]
33. Karjanto, N.; Van Groesen, E. Derivation of the NLS breather solutions using displaced phase-amplitude variables. *arXiv* **2011**, arXiv:1110.4704.
34. Karjanto, N. Bright soliton solution of the nonlinear Schrödinger equation: Fourier spectrum and fundamental characteristics. *Mathematics* **2022**, *10*, 4559. [CrossRef]
35. Karjanto, N. On spatial Fourier spectrum of rogue wave breathers. *Math. Methods Appl. Sci.* **2023**, *46*, 3405–3421. [CrossRef]
36. Karjanto, N. Mathematical Aspects of Extreme Water Waves. Ph.D. Thesis, Universiteit Twente, Enschede, The Netherlands, 2020. [CrossRef]
37. Karjanto, N.; Van Groesen, E. Mathematical physics properties of waves on finite background. In *Handbook of Solitons: Research, Technology and Applications*; Lang, S.P., Bedore, H., Eds.; Nova Science Publishers: Hauppauge, NY, USA, 2009; Chapter 14, pp. 501–539. [CrossRef]
38. Akter, J.; Akbar, M.A. Exact solutions to the Benney–Luke equation and the Phi-4 equations by using modified simple equation method. *Results Phys.* **2015**, *5*, 125–130. [CrossRef]
39. Pego, R.L.; Quintero, J.R. Two-dimensional solitary waves for a Benney–Luke equation. *Phys. D Nonlinear Phenom.* **1999**, *132*, 476–496. [CrossRef]
40. Benney, D.J.; Luke, J.C. On the interactions of permanent waves of finite amplitude. *J. Math. Phys.* **1964**, *43*, 309–313. [CrossRef]
41. Quintero, J.R.; Grajales, J.C.M. Instability of solitary waves for a generalized Benney–Luke equation. *Nonlinear Anal. Theory Methods Appl.* **2008**, *68*, 3009–3033. [CrossRef]
42. Wang, H. Lump and interaction solutions to the (2+ 1)-dimensional Burgers equation. *Appl. Math. Lett.* **2018**, *85*, 27–34. [CrossRef]
43. Ren, B.; Lin, J.; Lou, Z.M. A new nonlinear equation with LS, lump periodic, and lump-periodic-soliton solutions. *Complexity* **2019**, *2019*, 4072754. [CrossRef]
44. Yusuf, A.; Sulaiman, T.A.; Khalil, E.M.; Bayram, M.; Ahmad, H. Construction of multi-wave complexiton solutions of the Kadomtsev-Petviashvili equation via two efficient analyzing techniques. *Results Phys.* **2021**, *21*, 103775. [CrossRef]
45. Wang, K.J. Multi-wave complexiton, multi-wave, interaction-wave and the travelling wave solutions to the (2 + 1)-dimensional Boiti–Leon–Manna–Pempinelli equation for the incompressible fluid. *Pramana* **2024**, *98*, 47. [CrossRef]
46. Islam, S.R.; Khan, K.; Woadud, K.A.A. Analytical Studies on the Benney–Luke Equation in Mathematical Physics. *Waves Random Complex Media* **2018**, *28*, 300–309 [CrossRef]
47. Ibrahim, I.A.; Taha, W.M.; Noorani, M.S.M. Homogenous balance method for solving exact solutions of the nonlinear Benny-Luke equation and Vakhnenko-Parkes equation. *Zanco J. Pure Appl. Sci.* **2019**, *31*, 52–56.
48. Triki, H.; Yildirim, A.; Hayat, T.; Aldossary, O.M.; Biswas, A. Shock wave solution of the Benney-Luke equation. *Rom. J. Phys.* **2012**, *57*, 1029–1034.
49. Ablowitz, M.J.; Curtis, C.W. Conservation laws and non-decaying solutions for the Benney–Luke equation. *Proc. R. Soc. Math. Phys. Eng. Sci.* **2013**, *469*, 20120690. [CrossRef]
50. Hussain, A.; Usman, M.; Zaman, F.D.; Ibrahim, T.F.; Dawood, A.A. Symmetry analysis, closed-form invariant solutions and dynamical wave structures of the Benney-Luke equation using optimal system of Lie subalgebras. *Chin. J. Phys.* **2023**, *84*, 66–88. [CrossRef]
51. Grajales, J.C.M. Instability and long-time evolution of cnoidal wave solutions for a Benney–Luke equation. *Int. J. Non-Linear Mech.* **2009**, *44*, 999–1010. [CrossRef]